iScience

Article

The mesenteric adipokine SFRP5 alleviated intestinal epithelial apoptosis improving barrier dysfunction in Crohn's disease

Graphical abstract

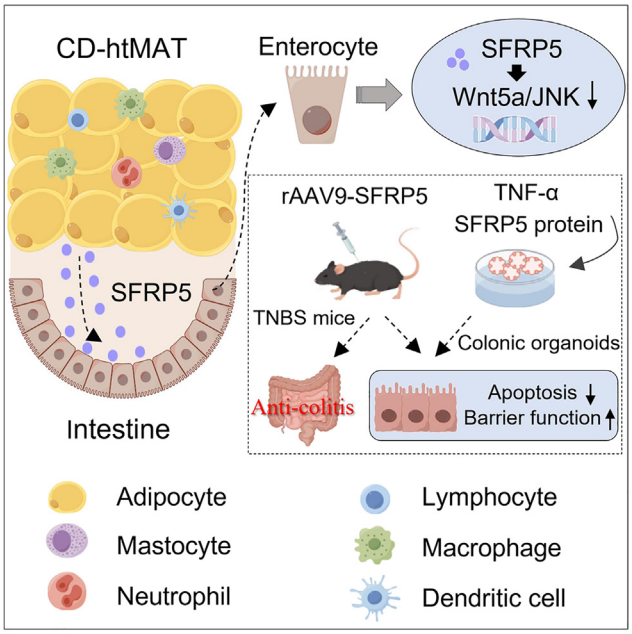

Highlights

- The adipokine SFRP5 was increased in the htMAT of CD patients
- SFRP5 has protective effects on enterocytes apoptosis and barrier dysfunction
- SFRP5 may ameliorative CD enteritis by inhibiting Wnt/JNK signaling
- Intestinal barrier may be a possible pathway for MAT to influence CD enteritis

Authors

Xiaofeng Zhang, Lugen Zuo, Xue Song, ..., Zhijun Geng, Jing Li, Jianguo Hu

Correspondence

jghu9200@163.com

In brief

Cell biology; Cancer

Zhang et al., 2024, iScience *27*, 111517
December 20, 2024
https://doi.org/10.1016/j.isci.2024.111517

CellPress

iScience

CellPress
OPEN ACCESS

Article

The mesenteric adipokine SFRP5 alleviated intestinal epithelial apoptosis improving barrier dysfunction in Crohn's disease

Xiaofeng Zhang,[1,2,3,7] Lugen Zuo,[2,3,4,7] Xue Song,[1,2,3,7] Wenjing Zhang,[5] Zi Yang,[4] Zhiyuan Wang,[6] Yibing Guo,[6] Sitang Ge,[2,3,4] Lian Wang,[4] Yueyue Wang,[2,3,5] Zhijun Geng,[1,2,3] Jing Li,[2,3,5] and Jianguo Hu[2,3,5,8,*]

[1]Department of Central Laboratory, First Affiliated Hospital of Bengbu Medical University, Bengbu, China
[2]Anhui Province Key Laboratory of Basic and Translational Research of Inflammation-related Diseases, Bengbu, China
[3]Inflammatory Bowel Disease Research Center, First Affiliated Hospital of Bengbu Medical University, Bengbu, China
[4]Department of Gastrointestinal Surgery, First Affiliated Hospital of Bengbu Medical University, Bengbu, Anhui, China
[5]Department of Clinical Laboratory, First Affiliated Hospital of Bengbu Medical University, Bengbu, China
[6]Clinical Medical College, Bengbu Medical University, Bengbu, China
[7]These authors contributed equally
[8]Lead contact
*Correspondence: jghu9200@163.com
https://doi.org/10.1016/j.isci.2024.111517

SUMMARY

The hypertrophic mesenteric adipose tissue (htMAT) of Crohn disease (CD) participates in inflammation through the expression of adipokines, but the exact mechanism of this action in the intestine is unknown. Here, we analyzed the expression of secreted frizzled-related protein 5 (SFRP5), an adipokine with cytoprotective effects, in htMAT and its role in CD. The results of this study revealed that the level of SFPR5 increased in the diseased MAT (htMAT) of CD patients and aggregated among intestinal epithelial cells in the diseased intestine and that it could ameliorate intestinal barrier dysfunction in tumor necrosis factor alpha (TNF-α)-stimulated colonic organoids and 2,4,6-trinitrobenzenesulfonic acid (TNBS)-induced mice at least in part through the inhibition of Wnt5a-mediated apoptosis in epithelial cells. This study elucidates possible mechanisms by which mesenteric adipokines influence the progression of enteritis and provides a new theoretical basis for the treatment of CD via the mesenteric pathway.

INTRODUCTION

Crohn disease (CD) belongs to inflammatory bowel disease characterized by body-weight-independent hypertrophic mesenteric adipose tissue (htMAT), which interacts with the intestine to influence CD progression.[1–3] Although crosstalk between the intestine and htMAT has long been recognized, the mechanism by which htMAT affects enteritis remains unclear. Focusing on this interaction is expected to provide new strategies for CD therapy.

Accumulating evidence suggests that CD-htMAT is associated with disease activity and increases the risk of complications and postoperative recurrence.[4–7] Recently, two well-designed studies showed that translocated gut bacteria and activated intestinal muscle cells drive the formation of mesenteric adipose tissue (MAT) lesions, which also provided strong evidence of an interaction between the intestine and htMAT in CD.[8,9] As the primary component of adipose tissue, adipocytes not only play a role in energy storage but also participate in regulating metabolism and the inflammatory response by secreting adipokines.[10–12] Our previous research confirmed that adipocytes in htMAT are characterized by functional impairments, with low lipid metabolism and proinflammatory endocrine features.[13] More importantly, we found that regulating adipokine levels could ameliorate htMAT lesions while ameliorating enteritis in CD model mice, but the specific pathways and mechanisms involved remain largely unknown.[14,15] The intestinal barrier plays an important role in maintaining intestinal health and protecting against pathogen infections.[16] Several previous studies have documented intestinal barrier dysfunction in patients with CD, as evidenced by the disruption of tight junctions (TJs) and increased epithelial permeability.[17,18] Notably, intestinal barrier dysfunction is an important factor maintaining chronic recurrent intestinal inflammation in CD and is an effective therapeutic target, as reported in previous studies, including ours.[19,20] However, whether the intestinal barrier serves as an intermediate link through which mesenteric adipokines affect intestinal inflammation is not clear.

Secretory frizzled-related protein 5 (SFRP5) is an adipokine that is expressed mainly in white adipose tissue and can play a protective role in various pathological processes by antagonizing apoptosis.[21,22] For example, treatment with SFRP5 not only inhibits cardiomyocyte apoptosis in diabetic mice with myocardial infarction but also counteracts ox-LDL-induced

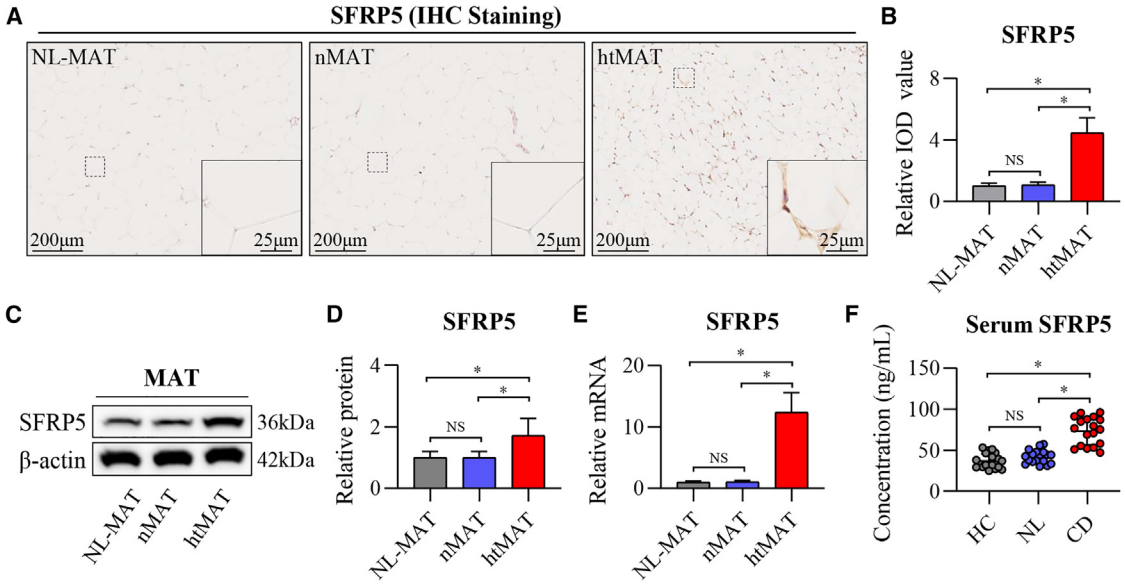

Figure 1. The adipokine SFRP5 was increased in the htMAT of CD patients

(A) Representative image of IHC staining showing that SFRP5 expression was elevated in htMAT but was only visible in NL-MAT and nMAT.

(B) Quantitative analysis of the results of the IHC staining for SFRP5.

(C and D) The level of the SFRP5 protein in MAT was detected by WB.

(E) The RT-qPCR result of SFRP5 in MAT.

(F) The levels of SFRP5 in the serum of humans were determined by enzyme-linked immunosorbent assay (ELISA). CD, Crohn disease; NL, colon cancer; HC, healthy control; MAT, mesenteric adipose tissue; htMAT, hypertrophic MAT in patients with CD; nMAT, normal MAT in patients with CD; NL-MAT, normal MAT in patients with colon cancer. $N = 18$ per group. The data are presented as the mean ± SD. ANOVA (Tukey's multiple test) was used for comparison of measurement data. $^{*}p < 0.05$. NS, not significant.

apoptosis in human umbilical vein endothelial cells (HUVECs) in the context of obesity.[23,24] Based on the fact that excessive apoptosis in intestinal epithelial cells is an important pathway and mechanism for intestinal barrier dysfunction in CD,[7,25,26] we hypothesized that the adipokine SFRP5, which has antiapoptotic effects, may mediate the effects of htMAT on CD-related intestinal barrier dysfunction and enteritis.

In the present study, using specimens from CD patients, we revealed that the adipokine SFRP5 was highly expressed in htMAT, accumulated in the diseased intestinal mucosa, and was negatively correlated with the proportion of apoptotic intestinal epithelial cells. In *ex vivo* experiments, SFRP5 exerted a direct antagonistic effect on tumor necrosis factor alpha (TNF-α)-induced intestinal epithelial cell apoptosis in mouse colonic organoids and protected against barrier dysfunction. We further demonstrated that SFRP5 antagonized intestinal epithelial cell apoptosis to protect against intestinal barrier injury and alleviate TNBS-induced CD-like colitis. Mechanistically, the antiapoptotic effect of SFRP5 on enterocytes at least partly involved the inhibition of Wnt5a signaling.

RESULTS

The adipokine SFRP5 was increased in the htMAT of CD patients

We first examined the expression of the adipokine SFRP5 using immunohistochemical (IHC) staining and found that it was abundant in htMAT but was only detectable in NL-MAT and nMAT (Figures 1A and 1B), as well as in the subcutaneous and omental adipose tissue from all groups (Figure S1). The results were confirmed by western blot (WB) (Figures 1C and 1D) and RT-qPCR (Figure 1E). We also detected increased levels of SFRP5, which is an exocrine protein, in the serum of patients with CD compared with those of patients with colon cancer and healthy controls (Figure 1F).

These results indicated that the secreted adipokine SFRP5 was highly expressed in CD-htMAT and was released into the peripheral blood.

SFRP5 highly accumulated among intestinal epithelial cells and may be related to epithelial cell apoptosis

Given the increased SFRP5 levels in CD-htMAT and serum, we were curious if it affects the intestine. As shown by H&E staining in Figure S2, there were a large infiltration of inflammatory cells in the diseased intestine adjacent to htMAT (I-htMAT), whereas only a few were seen in the normal intestine adjacent to NL-MAT (I-NL-MAT) and nMAT (I-nMAT). Interestingly, IHC staining revealed that SFRP5 was detected in the I-htMAT, most of which was distributed among intestinal epithelial cells (red arrow), whereas SFRP5 was hardly detected in the I-NL-MAT and I-nMAT (Figures 2A and 2B). These results were further confirmed by WB (Figures 2C and 2D). Moreover, the SFRP5 protein levels in htMAT were significantly positively correlated with the levels in I-htMAT (Figure 2E). These results, combined with the increased SFRP5 in the serum of CD patients, indicate that SFRP5 may act on the intestine via paracrine and/or endocrine pathways.

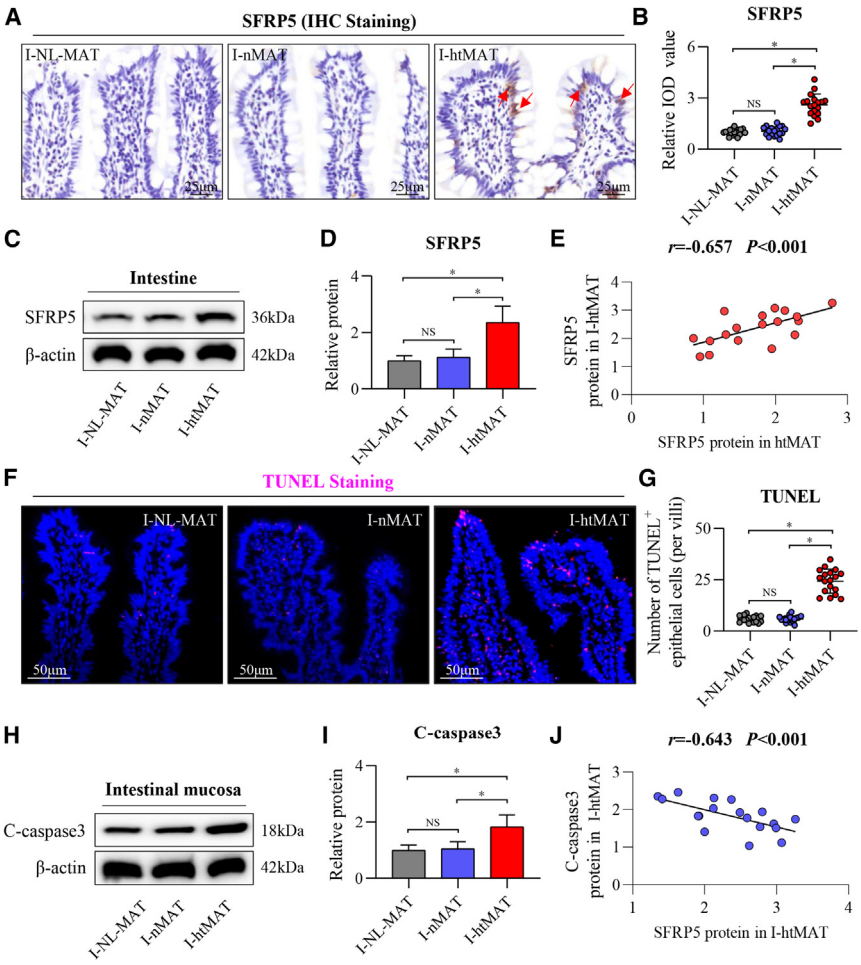

Figure 2. SFRP5 highly accumulated among intestinal epithelial cells and may be related to epithelial cell apoptosis

(A and B) Representative image of IHC staining showing the accumulation of SFRP5 in the diseased intestine and the results of the corresponding quantitative analysis.

(C and D) The SFRP5 protein level in the intestinal mucosa was determined by WB.

(E) Correlation analysis of SFRP5 protein levels (tested by WB) in the intestinal mucosa and htMAT.

(F and G) Representative image of TUNEL staining of the intestine and results of the corresponding quantitative analysis.

(H–J) C-caspase3 protein levels were measured by WB and correlated with SFRP5 protein levels (tested via WB) in the diseased intestinal mucosa of CD patients. I-htMAT, diseased intestine in patients with CD; I-nMAT, normal intestine in patients with CD; I-NL-MAT, normal intestine in patients with colon cancer; C-caspase3, cleaved caspase3. N = 18 per group. The data are presented as the mean ± SD. ANOVA (Tukey's multiple test) was used for comparison of measurement data. *$p < 0.05$. NS, not significant.

Due to the increase of SFRP5 among intestinal epithelial cells of I-htMAT and its antiapoptotic effect have been reported recently,[23] and we attempted to analyze the relationship between the SFRP5 level and apoptosis in intestinal epithelial cells. As expected, the proportion of apoptotic intestinal epithelial cells was significantly increased in the I-htMAT, as shown by TUNEL staining, whereas few apoptotic cells were detected and distributed mostly at the top of the intestinal villi in the I-NL-MAT and I-nMAT (Figures 2F and 2G). Immunofluorescence (IF) staining of I-htMAT suggested that the apoptotic marker C-caspase3 was concentrated in the SFRP5^{low} region, whereas the signal was attenuated in the SFRP5^{high} region (Figure S3).

The increased C-caspase3 level in I-htMAT was also confirmed by WB (Figures 2H and 2I), which was intriguingly negatively correlated with the SFRP5 level (tested by WB; Figure 2J).

It seems that the increased SFRP5 level in the I-htMAT may be associated with the apoptosis of intestinal epithelial cells in CD.

SFRP5 ameliorated intestinal epithelial apoptosis in the TNF-α-stimulated colonic organoids

Mouse colonic organoids were used to analyze the direct effect of SFRP5 on the apoptosis of intestinal epithelial cells. As shown in Figures 3A–3C, TNF-α significantly decreased the growth of colonic organoids, as evidenced by the decrease in size and budding number; surprisingly, these changes were almost eliminated by treatment with SFRP5. Furthermore, SFRP5 treatment significantly decreased TNF-α-induced intestinal epithelial cell death in the organoids, as evaluated by propidium iodide (PI) staining (Figures 3D and 3E). In addition, IF staining revealed that SFRP5 significantly relieved intestinal epithelial cell apoptosis in TNF-α-induced organoids, as evidenced by decreased levels of C-caspase3 (Figures 3F and 3G). A similar result was further confirmed by WB (Figures 3H and 3I).

Consequently, SFRP5 could directly antagonize inflammation-induced apoptosis in intestinal epithelial cells.

SFRP5 protected against intestinal barrier dysfunction in TNF-α-stimulated colonic organoids

Epithelial cell apoptosis is a key cause of intestinal barrier injury, which is one of the mechanisms that maintains chronic recurrent enteritis in CD.[27] Given the antiapoptotic effect of SFRP5, we further analyzed whether it could protect the intestinal barrier and found that SFRP5 could attenuate the increase in the permeability of colonic organoids to macromolecules (FD4) triggered by TNF-α stimulation (Figures 4A and 4B). SFRP5 also ameliorated the reduction in TEER caused by TNF-α stimulation in the colonic organoids (Figure 4C). In addition, IF staining revealed that SFRP5 maintained the loss of ZO-1 and Claudin-1 in the TNF-α-stimulated colonic organoids (Figure 4D), which was further confirmed by WB (Figures 4E–4G).

Thus, the anti-epithelial apoptotic effect of SFRP5 at least benefited intestinal barrier injury in the context of CD.

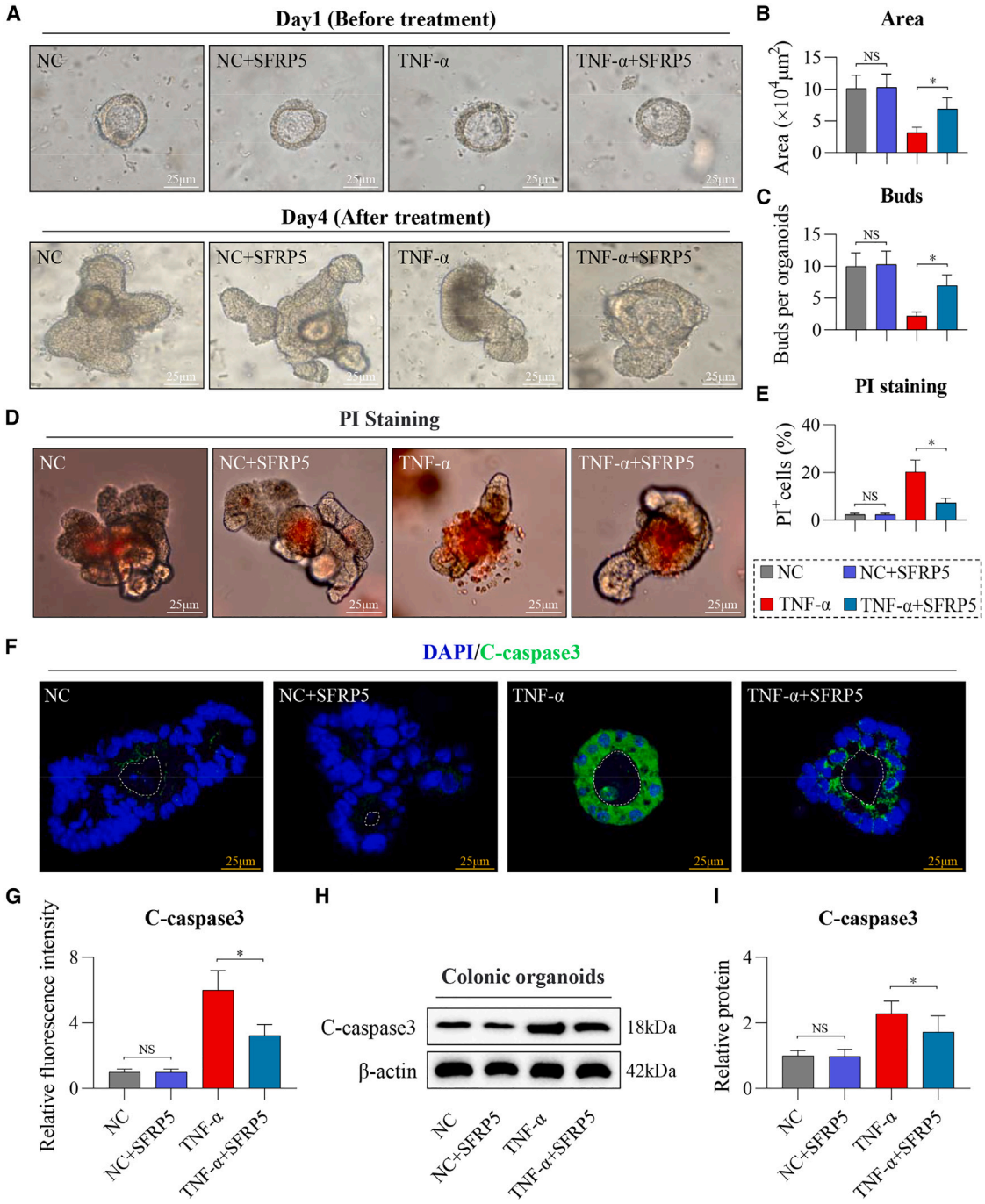

Figure 3. SFRP5 ameliorated intestinal epithelial apoptosis in TNF-α-stimulated colonic organoids

(A) Representative bright-field images of organoid growth.

(B and C) The area and budding number of the organoids were quantitatively analyzed.

(D and E) Representative images of PI staining and the results of corresponding quantitative analysis.

(F and G) Representative IF staining for the apoptosis marker C-caspase3 (green) and the results of the corresponding quantitative analysis.

(H and I) The C-caspase3 protein level was detected by WB. PI, propidium iodide. C-caspase3, cleaved caspase3. $N = 6$ per group. The data are presented as the mean ± SD. ANOVA (Tukey's multiple test) was used for comparison of measurement data. $^{*}p < 0.05$. NS, not significant.

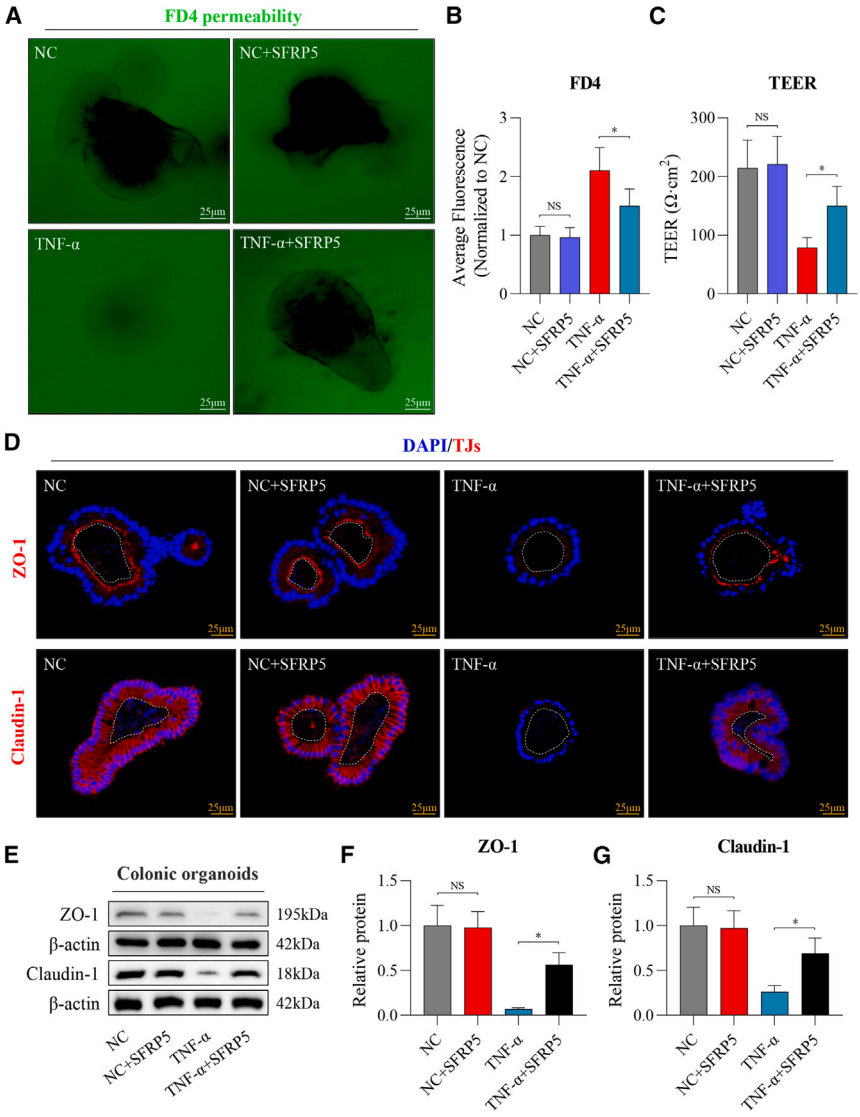

Figure 4. SFRP5 protected against intestinal barrier dysfunction in TNF-α-stimulated colonic organoids

(A and B) Representative images of FD4 permeability and results of the corresponding quantitative analysis.

(C) The TEER value of intestinal epithelial cells.

(D) Representative IF staining of TJs protein (ZO-1 and Claudin-1; red).

(E–G) The ZO-1 and Claudin-1 protein levels were detected by WB. FD4, fluorescein isothiocyanate-dextran [4 kDa]; TEER, transepithelial electrical resistance; TJs, tight junctions; ZO-1, zonula occludens-1. $N = 6$ per group. The data are presented as the mean ± SD. ANOVA (Tukey's multiple test) was used for comparison of measurement data. $^{*}p < 0.05$. NS, not significant.

SFRP5 antagonized epithelial cells apoptosis protecting barrier injury may be associated with the inhibition of Wnt5a/JNK signaling in TNF-α-stimulated colonic organoids

Inspired by a previous report that SFRP5 inhibits Wnt5a signaling to antagonize cardiomyocyte apoptosis,[24] we further explored the possible mechanism of the antiapoptotic effect of SFRP5 on intestinal epithelial cells. IF staining and WB analysis revealed that TNF-α stimulation increased Wnt5a expression in colonic organoids, which was largely inhibited by SFRP5. Moreover, SFRP5 also regulated the levels of apoptosis-regulating signaling factors downstream of Wnt5a (downregulation of p-JNK and upregulation of Bcl2) by WB. Importantly, the Wnt5a-specific agonist (Foxy-5) almost abolished the inhibitory effect of SFRP5 on Wnt5a signaling (Figures 5A–5E). Importantly, similar results were obtained in Caco2 cells (Figure S4). Furthermore, the antiapoptotic (Figures 5F and 5G) and barrier protection (Figures 5H–5L) effects of SFRP5 on TNF-α-stimulated colonic organoids were largely abolished by Foxy-5.

Collectively, the aforementioned results suggest that the regulation of intestinal epithelial cell apoptosis by SFRP5 is at least partially related to Wnt5a/JNK signaling.

SFRP5 ameliorated intestinal epithelial apoptosis in TNBS-induced mice

Next, we analyzed the effects of SFRP5 on intestinal epithelial cell apoptosis in TNBS-induced mice. We established a mouse model with upregulated SFRP5 expression in the mesentery using rAAV9-SFPR5 (Figure S5), and TUNEL staining revealed that TNBS-induced apoptosis in intestinal epithelial cells was significantly reduced by rAAV9-SFRP5 treatment (Figures 6A and 6B). Moreover, rAAV9-SFRP5 treatment significantly decreased the levels of C-caspase3 in the colonic mucosa of TNBS-induced mice, as detected by WB (Figures 6C and 6D).

These findings suggest that SFRP5 could inhibit apoptosis of intestinal epithelial cells in TNBS-induced mice *in vivo*.

SFRP5 improved intestinal barrier dysfunction in TNBS-induced mice

Motivated by the aforementioned findings, the role of SFRP5 in the intestinal barrier in TNBS-induced mice was further explored, and we found that the epithelial barrier was tightened in rAAV9-SFRP5-treated TNBS-induced mice, as evidenced by the decreased serum levels of I-FABP (Figure 7A), colonic macromolecular permeability (Figure 7B), and increased colonic TEER (Figure 7C). Moreover, treatment with rAAV9-SFRP5 significantly reduced the serum bacterial 16S rDNA level (Figure 7D) and the ratio of bacterial translocation in the mesenteric lymph nodes (MLNs), liver, and spleen of TNBS-induced mice (Figure S6). As presented in Figure 7E,

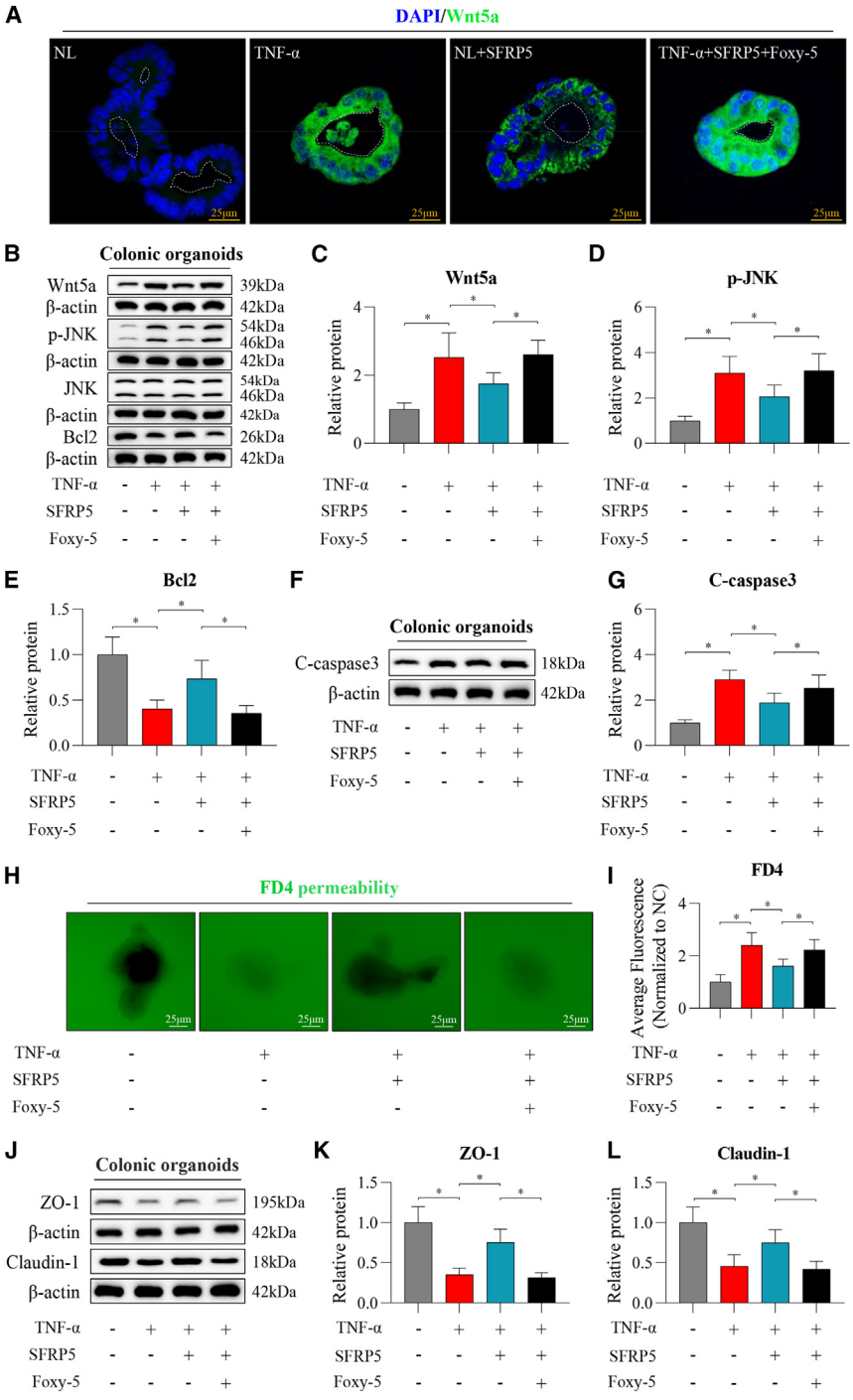

Figure 5. SFRP5 antagonized epithelial cells apoptosis protecting barrier injury may be associated with the inhibition of Wnt5a/JNK signaling in TNF-α-stimulated colonic organoids

(A) Representative IF labeling of Wnt5a (green).

(B–E) The levels of Wnt5a and its downstream signaling molecules (p-JNK and Bcl2) were detected via WB.

(F and G) The levels of C-caspase3 were detected by WB.

(H and I) Organoid permeability to FD4.

(J–L) The ZO-1 and Claudin-1 protein levels were examined by WB. FD4, fluorescein isothiocyanate-dextran (4 kDa); ZO-1, zonula occludens-1; C-caspase3, cleaved caspase3. $N = 6$ per group. The data are presented as the mean ± SD. ANOVA (Tukey's multiple test) was used for comparison of measurement data. $^{*}p < 0.05$.

Evidently, these data indicated that SFRP5 can attenuate intestinal epithelial apoptosis and intestinal barrier dysfunction in a model of CD-like colitis.

SFRP5 attenuated TNBS-induced CD-like colitis *in vivo*

The results described earlier motivated us to evaluate whether SFRP5 could ameliorate CD-like colitis, and we found that rAAV9-SFPR5 treatment significantly ameliorated colitis in TNBS-induced mice, as evidenced by improvements in the disease activity index (DAI) scores (Figure 8A), weight changes (Figure 8B), macroscopic damage scores (Figure 8C), colon shortening (Figures 8D and 8E), colonoscopy scores, and histological inflammation scores (Figures 8F–8I). In addition, the levels of proinflammatory cytokines (TNF-α, interleukin-6 [IL-6], IL-17A, and IL-1β) were significantly reduced in the colonic mucosa of TNBS-induced mice that received rAAV9-SFPR5, as determined by RT-qPCR (Figures 8J–8M) and ELISA (Figure S7).

Taken together, these results indicated that SFRP5 can ameliorate CD-like colitis *in vivo*.

the TEM results revealed that rAAV9-SFRP5 ameliorated the disrupted TJs structure, as indicated by the reduced electron density of TJs (arrows) and abnormal desmosomes (arrowheads). Furthermore, IF staining showed that rAAV9-SFRP5 ameliorated the loss of ZO-1 and Claudin-1 in the colonic mucosa of TNBS-induced mice (Figures 7F and 7G), and these results were further confirmed by WB (Figures 7H and 7I).

The protective effect of SFRP5 on CD-like colitis *in vivo* may be at least partially mediated by Wnt5a/JNK signaling

We investigated the mechanism by which SFRP5 affects CD-like colitis and found that rAAV9-SFRP5 treatment significantly downregulated Wnt5a and p-JNK levels and upregulated Bcl2 levels in the colonic mucosa of TNBS-induced mice and that

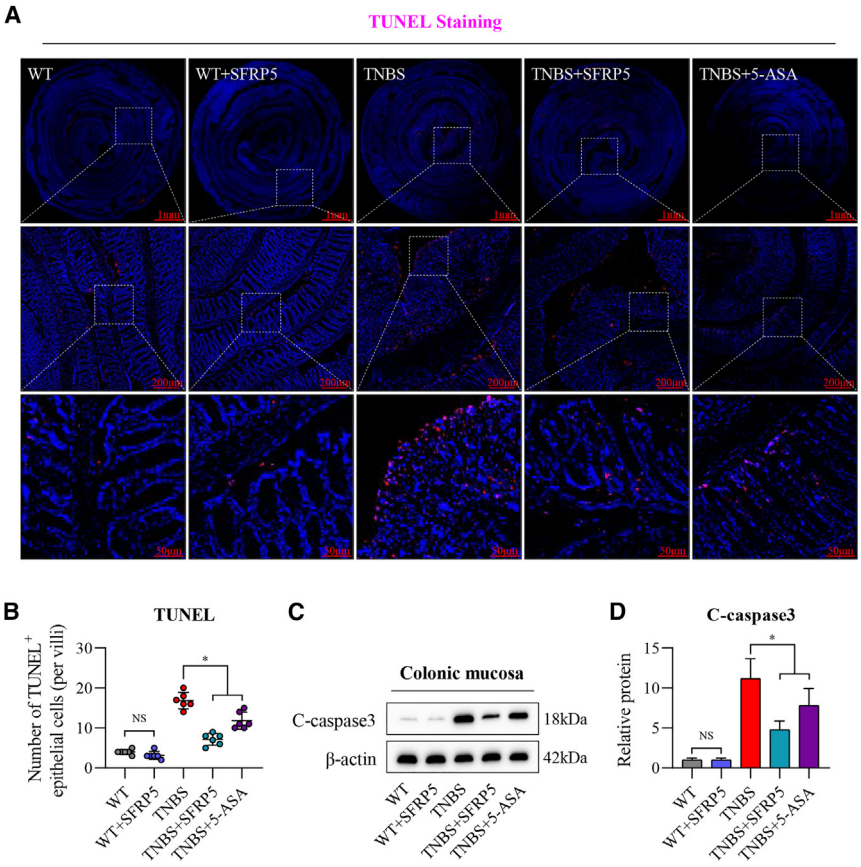

Figure 6. SFRP5 ameliorated intestinal epithelial apoptosis in TNBS-induced mice

(A and B) Representative TUNEL staining of colon tissue and corresponding quantitative analysis results.

(C and D) WB analysis of C-caspase3 in colonic mucosa. WT, wild-type; TNBS, 2,4,6-trinitrobenzenesulphonic acid; SFRP5, rAAV9-SFRP5. C-caspase3, cleaved caspase3. $N = 6$ per group. The data are expressed as the mean ± SD. ANOVA (Tukey's multiple test) was used for comparison of measurement data. $^{*}p < 0.05$. NS, not significant.

this effect was abolished by the Wnt5a-specific agonist Foxy-5 (Figures 9A–9D). Moreover, the protective effects of rAAV9-SFRP5 on the colon, including the levels of proinflammatory cytokines (TNF-α and IL-6; Figures 9E and 9F), DAI scores (Figure 9G), and histological inflammatory scores (Figures 9H and 9I), were also abolished by Foxy-5. Additionally, Foxy-5 eliminated the protective effects of rAAV9-SFRP5 on the intestinal barrier, as evidenced by the serum levels of FD4 (Figure 9J), colonic TEER values (Figure 9K), and the levels of ZO-1 and Claudin-1 (Figures 9L–9N). More critically, the antiapoptotic effects of rAAV9-SFRP5 on intestinal epithelial cells in TNBS-induced mice, such as the levels of C-caspase3 in the colonic mucosa, were also almost completely reversed by Foxy-5 (Figures 9O–9P).

Consequently, the beneficial effect of SFRP5 on CD-like colitis may be at least partly mediated by Wnt5a/JNK signaling.

DISCUSSION

Increasing evidence suggests that htMAT is not a passive bystander but rather participates in the inflammatory process of CD through the secretion of adipokines.[2] However, the exact pathways and mechanisms by which mesenteric adipokines affect enteritis are not clear. Previous studies, including ours, have reported that intestinal barrier dysfunction is an important therapeutic target for CD.[20,28] The present study examined whether the intestinal barrier is one of the focal locations through which mesenteric adipokines influence intestinal inflammation. The results of the study revealed that SFPR5 was highly expressed in htMAT of CD patients and aggregated among intestinal epithelial cells in the diseased intestine and that it could ameliorate intestinal barrier dysfunction in TNF-α-stimulated colonic organoids and TNBS-induced mice, at least in part, through the inhibition of Wnt5a-mediated apoptosis in epithelial cells.

To our knowledge, this report is the first to show that SFRP5 is highly expressed in CD-htMAT. Interestingly, SFRP5 was clearly identified in htMAT but not in normal MAT, as well as in subcutaneous and omental adipose tissue. We also detected increased SFRP5 levels in the serum of CD patients. More importantly, we observed an increased distribution of SFRP5 in the diseased intestine of CD patients but not in the normal intestine. Previous studies have shown that SFRP5 is a secreted adipokine that can be involved in the local or systemic regulation of metabolism and inflammation via circulatory or paracrine pathways.[29] A recent study indicated that the upregulation of SFRP5 expression improved insulin resistance and metabolic syndrome in high-fat-induced obese mice.[30] In addition to SFRP5, several other adipokines have been reported to be involved in disease progression; for example, high expression of leptin in perivascular adipose tissue accelerates the development of coronary atherosclerosis,[31–33] and adiponectin ameliorates insulin resistance in patients with type 2 diabetes.[34,35] Inspired by these studies, we hypothesized that SFRP5, which accumulates between intestinal epithelial cells, may be involved in CD colitis.

We elucidated the role of SFRP5 in CD by analyzing its effect on apoptosis in intestinal epithelial cells, as it has been previously reported to exert antiapoptotic effects on lipopolysaccharide (LPS)-induced chondrocytes[36] and a hypoxia-induced model of cardiac myocytes.[37] In the present study, we found that the levels of SFRP5 were negatively correlated with the proportion of apoptotic cells in the intestinal epithelium of CD patients. Moreover, SFRP5 antagonized intestinal epithelial cell apoptosis in TNF-α-stimulated colonic organoids *in vitro* and in

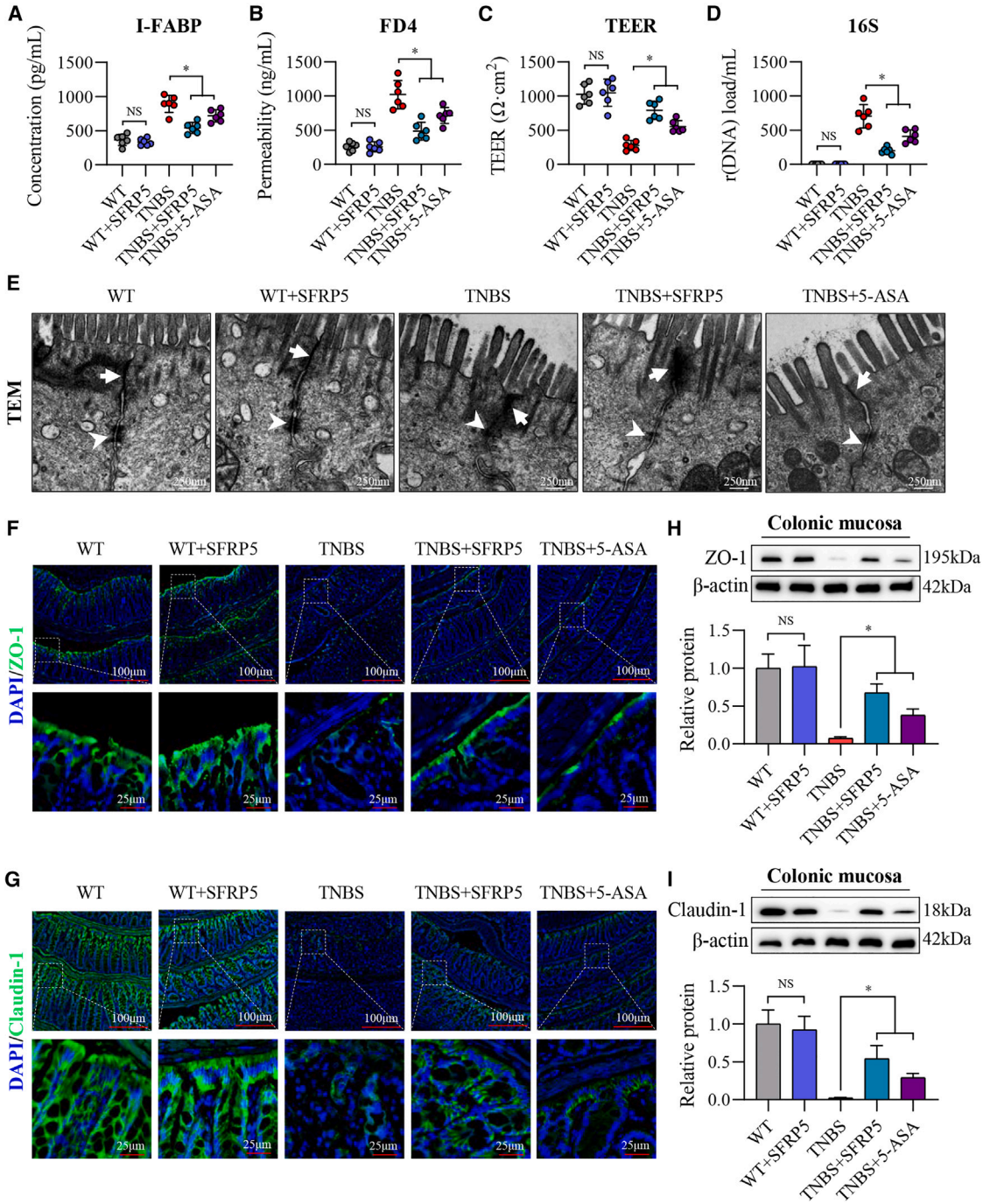

Figure 7. SFRP5 improved intestinal barrier dysfunction in TNBS-induced mice

(A and B) The serum levels of I-FABP and FD4 were measured.

(C) The colonic TEER value was detected.

(D) Analysis of bacterial 16S rDNA levels in serum.

(E) Representative TEM images of intercellular junctions in colon tissue (arrows, TJs; arrowheads, desmosomes).

(F and G) Representative images of IF staining of ZO-1 and Claudin-1 (green).

(H and I) The ZO-1 and Claudin-1 protein levels were detected by WB. WT, wild-type; TNBS, 2,4,6-trinitrobenzenesulfonic acid; SFRP5, rAAV9-SFRP5; I-FABP, intestinal fatty acid binding protein; FD4, fluorescein isothiocyanate-dextran (4 kDa); TEER, transepithelial electrical resistance; TEM, transmission electron microscopy; TJs, tight junctions; ZO-1, zonula occludens-1. $N = 6$ per group. The data are presented as the mean ± SD. ANOVA (Tukey's multiple test) was used for comparison of measurement data. $^{*}p < 0.05$. NS, not significant.

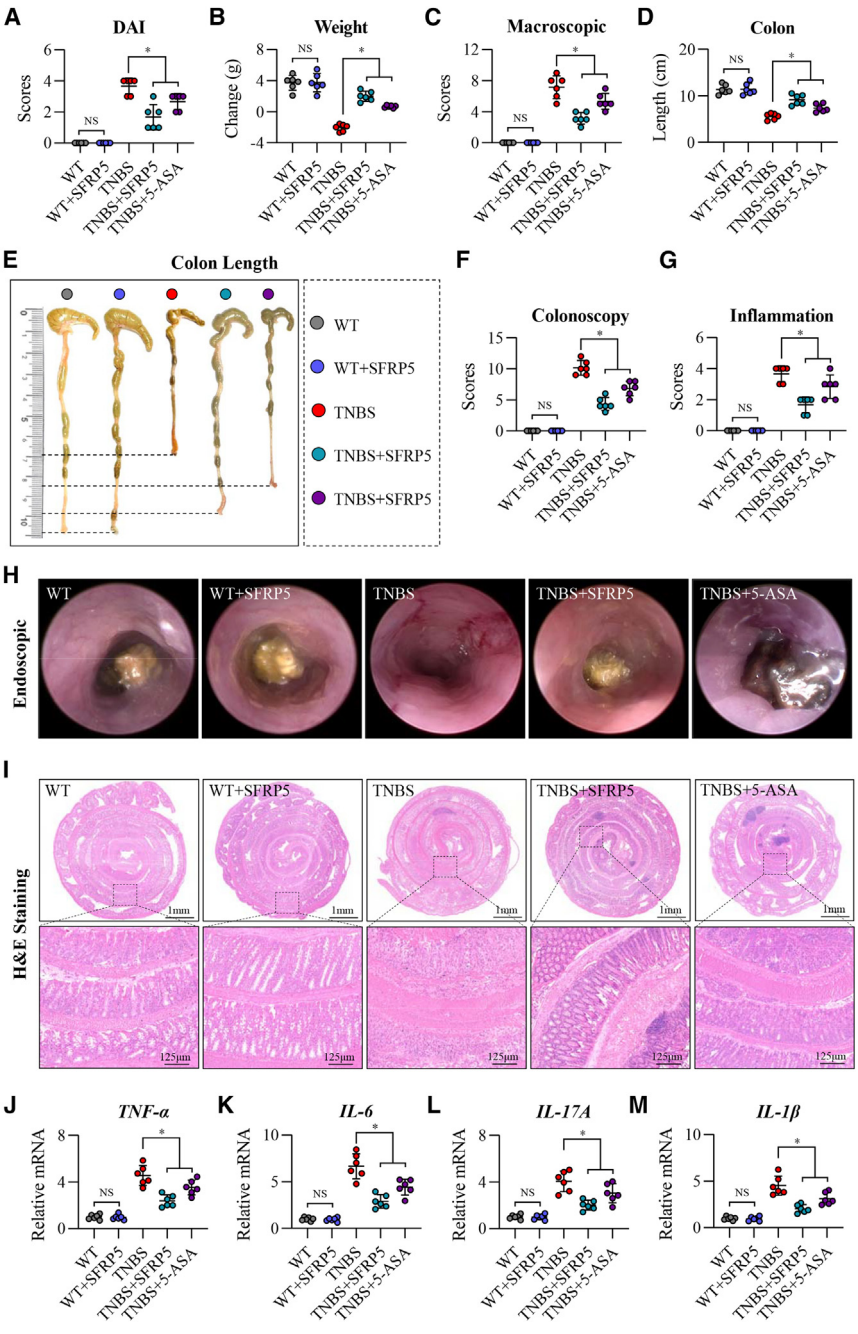

Figure 8. SFRP5 attenuated TNBS-induced CD-like colitis in vivo

(A) DAI scores, (B) weight changes, (C) macroscopic damage scores, and (D and E) colon lengths of each group.

(H) Representative images of a mouse endoscopy procedure and (F) corresponding colonoscopy scores.

(I) Representative images of H&E staining of the whole colon and (G) colonic histological inflammation scores. (J–M) The levels of pro-inflammatory cytokines were detected by RT-qPCR. WT, wild-type; TNBS, 2,4,6-trinitrobenzenesulfonic acid; SFRP5, rAAV9-SFRP5; DAI, disease activity index. $N = 6$ per group. The data are presented as the mean ± SD. ANOVA (Tukey's multiple test) was used for comparison of measurement data. *$p < 0.05$. NS, not significant.

TNBS-induced mice. Apoptosis is an important form of death in injured epithelial cells.[17] Excessive intestinal epithelial cell apoptosis is a key factor leading to intestinal barrier dysfunction and the subsequent initiation and maintenance of chronic enteritis; therefore, antagonizing epithelial cell apoptosis is one of the approaches for treating CD.[27,38]Intercellular TJs, between intestinal epithelial cells, not only maintain the polarity of the epithelium but also control the entry of bacteria, endotoxins, small molecules, and ions into the intestine.[16] ZO-1 and Claudin-1 are representative indicators of intestinal barrier integrity.[17] FD4 is widely used to study cell permeability, which reflects intestinal permeability to macromolecules,[20] and I-FABP is a small molecule protein expressed mainly in enterocytes, and its plasma level increases markedly in the early stages of intestinal barrier injury.[39] In both *in vitro* and *in vivo* studies, we have confirmed that SFRP5 prevents intestinal barrier dysfunction and, more importantly, that it alleviated TNBS-induced colitis in mice. However, the mechanism by which SFRP5 inhibits the apoptosis of intestinal epithelial cells is unknown.

To investigate the possible mechanisms and the antiapoptotic effects of SFRP5, we analyzed its role in Wnt5a signaling, as SFRP5/Wnt5a signaling could participate in the regulation of ox-LDL-induced apoptosis in HUVECs and hypoxia-/reoxygenation-induced apoptosis in neonatal rat ventricular myocytes.[23,40] In this study, we found that SFRP5 could inhibit the activation of Wnt5a signaling in TNF-α-stimulated colonic organoids and TNBS-induced mice. As reported previously, the activation of Wnt5a signaling can initiate the phosphorylation of Janus kinase (JNK), which in turn inhibits the activity of the antiapoptotic factor Bcl2.[41–43] In this study, we found that SFRP5 could inhibit the phosphorylation of JNK while increasing Bcl2 levels *in vivo* and *in vitro*. Interestingly, this effect was abrogated by the Wnt5a-specific agonist Foxy-5, as well as the antiapoptotic effects of SFRP5 on intestinal epithelial cells. As expected, Foxy-5 simultaneously eliminated the protective effects of SFRP5 on intestinal barrier dysfunction and colitis. Thus, SFRP5 antagonism of intestinal epithelial apoptosis plays a protective role in CD, at least in part through the inhibition of Wnt5a/JNK signaling.

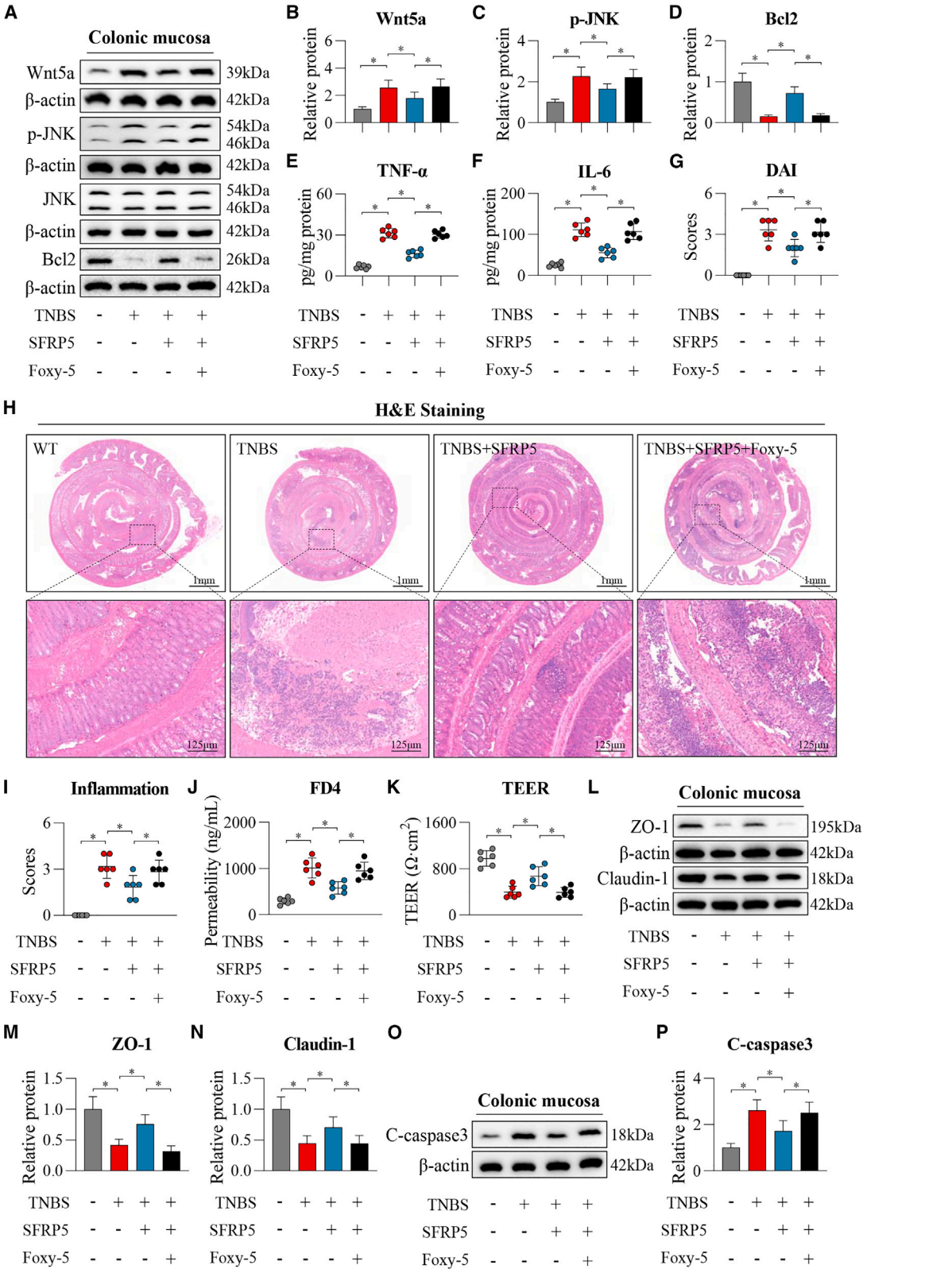

(legend on next page)

Recently, the important role of CD mesenteric lesions has been gradually emphasized, and several elegant studies have revealed that MAT lesions may be associated with intestinal bacterial translocation or the spread of intestinal inflammation.[8,9] Our group is trying to elucidate how the mesentery affects the progression of enteritis and found that improving the endocrine function of mesenteric adipocytes not only improves MAT lesions but also alleviates enteritis.[15] The present study further revealed that mesenteric adipokines may be involved in the development of CD enteritis by influencing apoptosis in intestinal epithelial cells, which provides a new perspective for a deeper understanding of the mechanism underlying the interaction between the mesentery and intestinal inflammation. In addition, our study revealed that SFRP5 has protective effects on intestinal epithelial cells and anti-inflammatory effects, expanding our understanding of its biological functions.

Overall, the present study revealed that the mesenteric adipokine SFRP5 could antagonize intestinal epithelial cell apoptosis and consequently protect against intestinal barrier dysfunction and colitis in CD, which was at least partially related to the inhibition of Wnt5a/JNK signaling. This study revealed a possible pathway by which MAT influences the progression of intestinal inflammation in the context of CD, deepened our understanding of the interaction between the mesentery and the intestine, and provided a new theoretical basis for CD therapy via the mesenteric pathway.

Limitations of the study

First, although TNBS-induced colitis mouse models can mimic intestinal inflammation in humans with CD,[44] more suitable animal models are still needed. Second, we revealed that SFRP5 could alleviate CD-like colitis and barrier dysfunction by inhibiting enterocyte apoptosis, but other pathways may have been overlooked. Finally, SFRP5 may regulate apoptosis in intestinal epithelial cells through multiple mechanisms, and Wnt5a signaling may only be one of these mechanisms.

RESOURCE AVAILABILITY

Lead contact

Further information and requests for resources should be directed to and will be fulfilled by the lead contact, Jianguo Hu (jghu9200@163.com).

Materials availability

This study did not generate new unique reagents and all materials in this study are commercially available.

Data and code availability

- Accession numbers are listed in the key resources table. All data reported in this article will be shared by the lead contact upon request.
- This paper does not report original code.
- Any additional information required to reanalyze the data reported in this paper is available from the lead contact upon request.

ACKNOWLEDGMENTS

This work was supported partly by funding from the National Natural Science Foundation of China [82370534 and 82070561], the Major Science and Technology Incubation plan of Bengbu Medical College [2020byfy003 and 2021byfy001], Excellent Scientific Research and Innovation Team Projects of Anhui Educational Committee [2023AH010067], Anhui Province University Outstanding Youth Research Project [2022AH020085 and 2023AH040289], Natural Science Research Project of Anhui Educational Committee [2023AH051952], the Research and Innovation Team of Bengbu Medical College [BYYFY2022TD002], the Natural Science Key Projects of Bengbu Medical College [2022byzd073], and the First Affiliated Hospital of Bengbu Medical College Science Fund for Outstanding Young Scholars [2019byyfyjq01 and 2019byyfyyq08].

AUTHOR CONTRIBUTIONS

X.Z., L.Z., X.S., and J.H. contributed to the study design, experiments, and manuscript drafting. W.Z., Z.Y., Z.W., Y.G., S.G., L.W., Y.W., Z.G., and J.L. contributed to the experiments and data analysis. J.H., X.Z., and L.Z. supervised the study, contributed to the critical the revision of the manuscript, and provided important intellectual content. All authors read and approved the final manuscript.

DECLARATION OF INTERESTS

The authors declare no financial conflicts of interest.

STAR★METHODS

Detailed methods are provided in the online version of this paper and include the following:

- KEY RESOURCES TABLE
- EXPERIMENTAL MODEL AND STUDY PARTICIPANT DETAILS
  - Human participants
  - Mice
  - Mouse colonic organoids
  - Caco2 cells
- METHOD DETAILS
  - Animal experimental design
  - Animal specimen collection and processing
  - Endoscopic colitis score
  - Histological analysis
  - Immunohistochemical [IHC] staining
  - RT-qPCR
  - ELISA

Figure 9. The protective effect of SFRP5 on CD-like colitis *in vivo* may be at least partially mediated by Wnt5a/JNK signaling

(A–D) The levels of Wnt5a, p-JNK, and Bcl2 in the colonic mucosa were analyzed by WB.

(E and F) The levels of TNF-α and IL-6 were detected via ELISA.

(G) DAI scores.

(H and I) Representative images of H&E staining of the whole colon and colonic inflammation scores.

(J and K) FD4 levels in the serum and colonic TEER values.

(L–P) The ZO-1, Claudin-1, and C-caspase3 protein levels were detected by WB. WT, wild-type; TNBS, 2,4,6-trinitrobenzenesulfonic acid; SFRP5, rAAV9-SFRP5; DAI, disease activity index; FD4, fluorescein isothiocyanate-dextran (4 kDa); TEER, transepithelial electrical resistance; ZO-1, zonula occludens-1; C-caspase3, cleaved caspase3. $N = 6$ per group. The data are presented as the mean ± SD. ANOVA (Tukey's multiple test) was used for comparison of measurement data. $^{*}p < 0.05$.

- Immunofluorescence [IF] analysis
- TUNEL staining
- Western bloting [WB]
- PI staining
- FD4 permeability analysis *in vivo*
- TEER measurement *in vivo*
- Measurement of 16S rDNA
- Bacterial translocation
- TEM analysis
- *Ex vivo* FD4 permeability assay
- TEER measurement in ex-vivo

- QUANTIFICATION AND STATISTICAL ANALYSIS

SUPPLEMENTAL INFORMATION

Supplemental information can be found online at https://doi.org/10.1016/j.isci.2024.111517.

Received: May 18, 2024
Revised: September 21, 2024
Accepted: November 28, 2024
Published: December 1, 2024

REFERENCES

1. Peyrin-Biroulet, L., Chamaillard, M., Gonzalez, F., Beclin, E., Decourcelle, C., Antunes, L., Gay, J., Neut, C., Colombel, J.F., and Desreumaux, P. (2007). Mesenteric fat in Crohn's disease: a pathogenetic hallmark or an innocent bystander. Gut *56*, 577–583. https://doi.org/10.1136/gut.2005.082925.
2. Li, Y., Zhu, W., Zuo, L., and Shen, B. (2016). The Role of the Mesentery in Crohn's Disease: The Contributions of Nerves, Vessels, Lymphatics, and Fat to the Pathogenesis and Disease Course. Inflamm. Bowel Dis. *22*, 1483–1495. https://doi.org/10.1097/MIB.0000000000000791.
3. Mao, R., Kurada, S., Gordon, I.O., Baker, M.E., Gandhi, N., McDonald, C., Coffey, J.C., and Rieder, F. (2019). The Mesenteric Fat and Intestinal Muscle Interface: Creeping Fat Influencing Stricture Formation in Crohn's Disease. Inflamm. Bowel Dis. *25*, 421–426. https://doi.org/10.1093/ibd/izy331.
4. Holt, D.Q., Moore, G.T., Strauss, B.J.G., Hamilton, A.L., De Cruz, P., and Kamm, M.A. (2017). Visceral adiposity predicts post-operative Crohn's disease recurrence. Aliment. Pharmacol. Ther. *45*, 1255–1264. https://doi.org/10.1111/apt.14018.
5. Sakurai, T., Katsuno, T., Saito, K., Yoshihama, S., Nakagawa, T., Koseki, H., Taida, T., Ishigami, H., Okimoto, K.I., Maruoka, D., et al. (2017). Mesenteric findings of CT enterography are well correlated with the endoscopic severity of Crohn's disease. Eur. J. Radiol. *89*, 242–248. https://doi.org/10.1016/j.ejrad.2016.10.022.
6. Althoff, P., Schmiegel, W., Lang, G., Nicolas, V., and Brechmann, T. (2019). Creeping Fat Assessed by Small Bowel MRI Is Linked to Bowel Damage and Abdominal Surgery in Crohn's Disease. Dig. Dis. Sci. *64*, 204–212. https://doi.org/10.1007/s10620-018-5303-1.
7. Meijer, B.J., Giugliano, F.P., Baan, B., van der Meer, J.H.M., Meisner, S., van Roest, M., Koelink, P.J., de Boer, R.J., Jones, N., Breitwieser, W., et al. (2020). ATF2 and ATF7 Are Critical Mediators of Intestinal Epithelial Repair. Cell. Mol. Gastroenterol. Hepatol. *10*, 23–42. https://doi.org/10.1016/j.jcmgh.2020.01.005.
8. Ha, C.W.Y., Martin, A., Sepich-Poore, G.D., Shi, B., Wang, Y., Gouin, K., Humphrey, G., Sanders, K., Ratnayake, Y., Chan, K.S.L., et al. (2020). Translocation of Viable Gut Microbiota to Mesenteric Adipose Drives Formation of Creeping Fat in Humans. Cell *183*, 666–683. https://doi.org/10.1016/j.cell.2020.09.009.
9. Mao, R., Doyon, G., Gordon, I.O., Li, J., Lin, S., Wang, J., Le, T.H.N., Elias, M., Kurada, S., Southern, B., et al. (2022). Activated intestinal muscle cells promote preadipocyte migration: a novel mechanism for creeping fat formation in Crohn's disease. Gut *71*, 55–67. https://doi.org/10.1136/gutjnl-2020-323719.
10. Giralt, M., Cereijo, R., and Villarroya, F. (2016). Adipokines and the Endocrine Role of Adipose Tissues. Handb. Exp. Pharmacol. *233*, 265–282. https://doi.org/10.1007/164_2015_6.
11. Kahn, C.R., Wang, G., and Lee, K.Y. (2019). Altered adipose tissue and adipocyte function in the pathogenesis of metabolic syndrome. J. Clin. Invest. *129*, 3990–4000. https://doi.org/10.1172/JCI129187.
12. Blaszczak, A.M., Jalilvand, A., and Hsueh, W.A. (2021). Adipocytes, Innate Immunity and Obesity: A Mini-Review. Front. Immunol. *12*, 650768. https://doi.org/10.3389/fimmu.2021.650768.
13. Zuo, L., Li, Y., Zhu, W., Shen, B., Gong, J., Guo, Z., Zhang, W., Wu, R., Gu, L., Li, N., and Li, J. (2016). Mesenteric Adipocyte Dysfunction in Crohn's Disease is Associated with Hypoxia. Inflamm. Bowel Dis. *22*, 114–126. https://doi.org/10.1097/MIB.0000000000000571.
14. Li, Y., Zuo, L., Zhu, W., Gong, J., Zhang, W., Guo, Z., Gu, L., Li, N., and Li, J. (2015). Telmisartan attenuates the inflamed mesenteric adipose tissue in spontaneous colitis by mechanisms involving regulation of neurotensin/microRNA-155 pathway. Biochem. Pharmacol. *93*, 461–469. https://doi.org/10.1016/j.bcp.2014.12.020.
15. Zuo, L., Ge, S., Ge, Y., Li, J., Zhu, B., Zhang, Z., Jiang, C., Li, J., Wang, S., Liu, M., et al. (2019). The Adipokine Metrnl Ameliorates Chronic Colitis in Il-10-/- Mice by Attenuating Mesenteric Adipose Tissue Lesions During Spontaneous Colitis. J. Crohns Colitis *13*, 931–941. https://doi.org/10.1093/ecco-jcc/jjz001.
16. Song, X., Huang, Q., Yang, Y., Ma, L., Liu, W., Ou, C., Chen, Q., Zhao, T., Xiao, Z., Wang, M., et al. (2023). Efficient Therapy of Inflammatory Bowel Disease (IBD) with Highly Specific and Durable Targeted Ta(2) C Modified with Chondroitin Sulfate (TACS). Adv. Mater. *35*, e2301585. https://doi.org/10.1002/adma.202301585.
17. Huang, Q., Yang, Y., Zhu, Y., Chen, Q., Zhao, T., Xiao, Z., Wang, M., Song, X., Jiang, Y., Yang, Y., et al. (2023). Oral Metal-Free Melanin Nanozymes for Natural and Durable Targeted Treatment of Inflammatory Bowel Disease (IBD). Small *19*, e2207350. https://doi.org/10.1002/smll.202207350.
18. Odenwald, M.A., and Turner, J.R. (2017). The intestinal epithelial barrier: a therapeutic target. Nat. Rev. Gastroenterol. Hepatol. *14*, 9–21. https://doi.org/10.1038/nrgastro.2016.169.
19. Chen, G., Ran, X., Li, B., Li, Y., He, D., Huang, B., Fu, S., Liu, J., and Wang, W. (2018). Sodium Butyrate Inhibits Inflammation and Maintains Epithelium Barrier Integrity in a TNBS-induced Inflammatory Bowel Disease Mice Model. EBioMedicine *30*, 317–325. https://doi.org/10.1016/j.ebiom.2018.03.030.
20. Zhang, X., Zuo, L., Geng, Z., Song, X., Li, J., Ge, S., Jiang, Y., Yang, Z., Liu, G., Zhao, Y., et al. (2022). Vindoline ameliorates intestinal barrier damage in Crohn's disease mice through MAPK signaling pathway. Faseb. J. *36*, e22589. https://doi.org/10.1096/fj.202200234RR.
21. Wang, C.P., Yu, T.H., Wu, C.C., Hung, W.C., Hsu, C.C., Tsai, I.T., Tang, W.H., Chung, F.M., Houng, J.Y., Lee, Y.J., and Lu, Y.C. (2018). Circulating secreted frizzled-related protein 5 and chronic kidney disease in patients with acute ST-segment elevation myocardial infarction. Cytokine *110*, 367–373. https://doi.org/10.1016/j.cyto.2018.04.009.
22. Zhou, W., Ye, C., Li, L., Liu, L., Wang, F., Yu, L., Zhou, F., Xiang, Y., Wang, Y., Yin, G., et al. (2020). Adipocyte-derived SFRP5 inhibits breast cancer cells migration and invasion through Wnt and epithelial-mesenchymal transition signaling pathways. Chin. J. Cancer Res. *32*, 347–360. https://doi.org/10.21147/j.issn.1000-9604.2020.03.06.
23. Liu, W., Ji, Y., Chu, H., Wang, M., Yang, B., and Yin, C. (2020). SFRP5 mediates downregulation of the wnt5a/caveolin-1/JNK signaling pathway. J. Endocrinol. *247*, 263–272. https://doi.org/10.1530/JOE-20-0328.
24. Ding, N., and Zheng, C. (2022). Secreted frizzled-related protein 5 promotes angiogenesis of human umbilical vein endothelial cells and alleviates myocardial injury in diabetic mice with myocardial infarction by

inhibiting Wnt5a/JNK signaling. Bioengineered *13*, 11656–11667. https://doi.org/10.1080/21655979.2022.2070964.

25. Bruewer, M., Luegering, A., Kucharzik, T., Parkos, C.A., Madara, J.L., Hopkins, A.M., and Nusrat, A. (2003). Proinflammatory cytokines disrupt epithelial barrier function by apoptosis-independent mechanisms. J. Immunol. *171*, 6164–6172. https://doi.org/10.4049/jimmunol.171.11.6164.

26. Wen, H., Zhang, X., Li, Q., Huang, J., Liu, G., Zhao, J., Liu, Y., Shen, L., Li, Y., Yang, K., et al. (2022). Ruscogenins Improve CD-Like Enteritis by Inhibiting Apoptosis of Intestinal Epithelial Cells and Activating Nrf2/NQO1 Pathway. Oxid. Med. Cell. Longev. *2022*, 4877275. https://doi.org/10.1155/2022/4877275.

27. Günther, C., Neumann, H., Neurath, M.F., and Becker, C. (2013). Apoptosis, necrosis and necroptosis: cell death regulation in the intestinal epithelium. Gut *62*, 1062–1071. https://doi.org/10.1136/gutjnl-2011-301364.

28. Zuo, L., Li, J., Ge, S., Ge, Y., Shen, M., Wang, Y., Zhou, C., Wu, R., and Hu, J. (2019). Bryostatin-1 ameliorated experimental colitis in Il-10(-/-) Mice by protecting the intestinal barrier and limiting immune dysfunction. J. Cell Mol. Med. *23*, 5588–5599. https://doi.org/10.1111/jcmm.14457.

29. Jaikanth, C., Gurumurthy, P., Indhumathi, T., and Cherian, K.M. (2017). Emergence of SFRP5 as a pleiotropic adipocytokine and its association with Wnt signaling pathways. Minerva Endocrinol. *42*, 280–289. https://doi.org/10.23736/S0391-1977.16.02232-X.

30. Ouchi, N., Higuchi, A., Ohashi, K., Oshima, Y., Gokce, N., Shibata, R., Akasaki, Y., Shimono, A., and Walsh, K. (2010). Sfrp5 is an anti-inflammatory adipokine that modulates metabolic dysfunction in obesity. Science *329*, 454–457. https://doi.org/10.1126/science.1188280.

31. Payne, G.A., Borbouse, L., Kumar, S., Neeb, Z., Alloosh, M., Sturek, M., and Tune, J.D. (2010). Epicardial perivascular adipose-derived leptin exacerbates coronary endothelial dysfunction in metabolic syndrome via a protein kinase C-beta pathway. Arterioscler. Thromb. Vasc. Biol. *30*, 1711–1717. https://doi.org/10.1161/ATVBAHA.110.210070.

32. Payne, G.A., Tune, J.D., and Knudson, J.D. (2014). Leptin-induced endothelial dysfunction: a target for therapeutic interventions. Curr. Pharmaceut. Des. *20*, 603–608. https://doi.org/10.2174/13816128113199990017.

33. Nosalski, R., and Guzik, T.J. (2017). Perivascular adipose tissue inflammation in vascular disease. Br. J. Pharmacol. *174*, 3496–3513. https://doi.org/10.1111/bph.13705.

34. Hotta, K., Funahashi, T., Bodkin, N.L., Ortmeyer, H.K., Arita, Y., Hansen, B.C., and Matsuzawa, Y. (2001). Circulating concentrations of the adipocyte protein adiponectin are decreased in parallel with reduced insulin sensitivity during the progression to type 2 diabetes in rhesus monkeys. Diabetes *50*, 1126–1133. https://doi.org/10.2337/diabetes.50.5.1126.

35. Yamauchi, T., and Kadowaki, T. (2013). Adiponectin receptor as a key player in healthy longevity and obesity-related diseases. Cell Metabol. *17*, 185–196. https://doi.org/10.1016/j.cmet.2013.01.001.

36. Sun, M., Wang, W., Min, L., Chen, C., Li, Q., and Weng, W. (2021). Secreted frizzled-related protein 5 (SFRP5) protects ATDC5 cells against LPS-induced inflammation and apoptosis via inhibiting Wnt5a/JNK pathway. J. Orthop. Surg. Res. *16*, 129. https://doi.org/10.1186/s13018-021-02260-5.

37. Huang, X., Yan, Y., Zheng, W., Ma, Y., Wang, X., Gong, W., and Nie, S. (2021). Secreted Frizzled-Related Protein 5 Protects Against Cardiac Rupture and Improves Cardiac Function Through Inhibiting Mitochondrial Dysfunction. Front. Cardiovasc. Med. *8*, 682409. https://doi.org/10.3389/fcvm.2021.682409.

38. Shao, M., Yan, Y., Zhu, F., Yang, X., Qi, Q., Yang, F., Hao, T., Lin, Z., He, P., Zhou, Y., et al. (2022). Artemisinin analog SM934 alleviates epithelial barrier dysfunction via inhibiting apoptosis and caspase-1-mediated pyroptosis in experimental colitis. Front. Pharmacol. *13*, 849014. https://doi.org/10.3389/fphar.2022.849014.

39. Sarikaya, M., Ergül, B., Doğan, Z., Filik, L., Can, M., and Arslan, L. (2015). Intestinal fatty acid binding protein (I-FABP) as a promising test for Crohn's disease: a preliminary study. Clin. Lab. *61*, 87–91. https://doi.org/10.7754/clin.lab.2014.140518.

40. Nakamura, K., Sano, S., Fuster, J.J., Kikuchi, R., Shimizu, I., Ohshima, K., Katanasaka, Y., Ouchi, N., and Walsh, K. (2016). Secreted Frizzled-related Protein 5 Diminishes Cardiac Inflammation and Protects the Heart from Ischemia/Reperfusion Injury. J. Biol. Chem. *291*, 2566–2575. https://doi.org/10.1074/jbc.M115.693937.

41. Dhanasekaran, D.N., and Reddy, E.P. (2017). JNK-signaling: A multiplexing hub in programmed cell death. Genes Cancer *8*, 682–694. https://doi.org/10.18632/genesandcancer.155.

42. Tong, S., Ji, Q., Du, Y., Zhu, X., Zhu, C., and Zhou, Y. (2019). Sfrp5/Wnt Pathway: A Protective Regulatory System in Atherosclerotic Cardiovascular Disease. J. Interferon Cytokine Res. *39*, 472–482. https://doi.org/10.1089/jir.2018.0154.

43. Rogers, S., and Scholpp, S. (2022). Vertebrate Wnt5a - At the crossroads of cellular signalling. Semin. Cell Dev. Biol. *125*, 3–10. https://doi.org/10.1016/j.semcdb.2021.10.002.

44. Wirtz, S., Popp, V., Kindermann, M., Gerlach, K., Weigmann, B., Fichtner-Feigl, S., and Neurath, M.F. (2017). Chemically induced mouse models of acute and chronic intestinal inflammation. Nat. Protoc. *12*, 1295–1309. https://doi.org/10.1038/nprot.2017.044.

45. Garcia-Carbonell, R., Wong, J., Kim, J.Y., Close, L.A., Boland, B.S., Wong, T.L., Harris, P.A., Ho, S.B., Das, S., Ernst, P.B., et al. (2018). Elevated A20 promotes TNF-induced and RIPK1-dependent intestinal epithelial cell death. Proc. Natl. Acad. Sci. USA *115*, E9192–E9200. https://doi.org/10.1073/pnas.1810584115.

46. Canesin, G., Evans-Axelsson, S., Hellsten, R., Krzyzanowska, A., Prasad, C.P., Bjartell, A., and Andersson, T. (2017). Treatment with the WNT5A-mimicking peptide Foxy-5 effectively reduces the metastatic spread of WNT5A-low prostate cancer cells in an orthotopic mouse model. PLoS One *12*, e0184418. https://doi.org/10.1371/journal.pone.0184418.

47. Spencer, D.M., Veldman, G.M., Banerjee, S., Willis, J., and Levine, A.D. (2002). Distinct inflammatory mechanisms mediate early versus late colitis in mice. Gastroenterology *122*, 94–105. https://doi.org/10.1053/gast.2002.30308.

48. Becker, C., Fantini, M.C., and Neurath, M.F. (2006). High resolution colonoscopy in live mice. Nat. Protoc. *1*, 2900–2904. https://doi.org/10.1038/nprot.2006.446.

49. Koelink, P.J., Wildenberg, M.E., Stitt, L.W., Feagan, B.G., Koldijk, M., van't Wout, A.B., Atreya, R., Vieth, M., Brandse, J.F., Duijst, S., and Te Velde, A.A. (2018). Development of Reliable, Valid and Responsive Scoring Systems for Endoscopy and Histology in Animal Models for Inflammatory Bowel Disease. Journal of Crohn's & colitis *12*, 794–803. https://doi.org/10.1093/ecco-jcc/jjy035.

50. Schultz, M., Tonkonogy, S.L., Sellon, R.K., Veltkamp, C., Godfrey, V.L., Kwon, J., Grenther, W.B., Balish, E., Horak, I., and Sartor, R.B. (1999). IL-2-deficient mice raised under germfree conditions develop delayed mild focal intestinal inflammation. Am. J. Physiol. *276*, G1461–G1472. https://doi.org/10.1152/ajpgi.1999.276.6.G1461.

51. Biskou, O., Meira de-Faria, F., Walter, S.M., Winberg, M.E., Haapaniemi, S., Myrelid, P., Söderholm, J.D., and Keita, Å.V. (2022). Increased Numbers of Enteric Glial Cells in the Peyer's Patches and Enhanced Intestinal Permeability by Glial Cell Mediators in Patients with Ileal Crohn's Disease. Cells *11*, 335. https://doi.org/10.3390/cells11030335.

52. Zhang, Y., Duan, C., Wu, S., Ma, J., Liu, Y., Li, W., Wang, T., Yang, L., Cheng, K., and Zhuang, R. (2022). Knockout of IL-6 mitigates cold water-immersion restraint stress-induced intestinal epithelial injury and apoptosis. Front. Immunol. *13*, 936689. https://doi.org/10.3389/fimmu.2022.936689.

53. Dong, W., Zhang, Z., Liu, Z., Liu, H., Wang, X., Bi, S., Wang, X., Ma, T., and Zhang, W. (2013). Protective effects of osthole, a natural derivative of

coumarin, against intestinal ischemia-reperfusion injury in mice. Int. J. Mol. Med. *31*, 1367–1374. https://doi.org/10.3892/ijmm.2013.1347.

54. Bode, K.J., Mueller, S., Schweinlin, M., Metzger, M., and Brunner, T. (2019). A fast and simple fluorometric method to detect cell death in 3D intestinal organoids. Biotechniques *67*, 23–28. https://doi.org/10.2144/btn-2019-0023.

55. Zuo, L., Li, Y., Wang, H., Wu, R., Zhu, W., Zhang, W., Cao, L., Gu, L., Gong, J., Li, N., and Li, J. (2014). Cigarette smoking is associated with intestinal barrier dysfunction in the small intestine but not in the large intestine of mice. J. Crohns Colitis *8*, 1710–1722. https://doi.org/10.1016/j.crohns.2014.08.008.

56. Jiang, W. (2018). A protocol for quantizing total bacterial 16S rDNA in plasma as a marker of microbial translocation in vivo. Cell. Mol. Immunol. *15*, 937–939. https://doi.org/10.1038/cmi.2018.3.

57. Patterson, L., Allen, J., Posey, I., Shaw, J.J.P., Costa-Pinheiro, P., Walker, S.J., Gademsey, A., Wu, X., Wu, S., Zachos, N.C., et al. (2020). Glucosylceramide production maintains colon integrity in response to Bacteroides fragilis toxin-induced colon epithelial cell signaling. Faseb. J. *34*, 15922–15945. https://doi.org/10.1096/fj.202001669R.

58. Cheng, Y., Hall, T.R., Xu, X., Yung, I., Souza, D., Zheng, J., Schiele, F., Hoffmann, M., Mbow, M.L., Garnett, J.P., and Li, J. (2022). Targeting uPA-uPAR interaction to improve intestinal epithelial barrier integrity in inflammatory bowel disease. EBioMedicine *75*, 103758. https://doi.org/10.1016/j.ebiom.2021.103758.

STAR★METHODS

KEY RESOURCES TABLE

REAGENT or RESOURCE	SOURCE	IDENTIFIER
Antibodies		
anti-SFRP5 antibody	Abcam	ab230425
anti-C-caspase3 antibody	Cell signaling	Cat# 9661; RRID: AB_2341188
anti-ZO-1 antibody	Abcam	ab307799
anti-Claudin-1 antibody	Abcam	Cat# ab307692; RRID: AB_3083082
anti-Wnt5a antibody	Stanta Santa Cruz	sc-365370
anti-JNK antibody	Cell Signaling	Cat# 9252; RRID: AB_2250373
anti-*p*-JNK antibody	Cell Signaling	Cat# 4668; RRID: AB_823588
anti-Bcl2 antibody	Abcam	Cat# ab182858; RRID: AB_2715467
goat anti-rabbit IgG H&L [HRP]	Abcam	Cat# ab6721; RRID: AB_955447
anti-β-actin antibody	Abcam	Cat# ab8226; RRID: AB_306371
Goat Anti-rabbit IgG H&L [FITC]	Abcam	Cat# ab6717; RRID: AB_955238
Goat Anti-Mouse IgG H&L [FITC]	Abcam	Cat# ab6785; RRID: AB_955241
Goat Anti-Rabbit IgG H&L [Alexa Fluor®555]	Abcam	Cat# ab150078; RRID: AB_2722519
Chemicals, peptides, and recombinant proteins		
TNBS	Sigma Aldrich	P2297
DAB	ZSGB-BIO	ZLI-9018
PBS	Solarbio	P1020
EDTA	Solarbio	E1170
Matrigel	Corning	356255
Organoid Growth Medium [Mouse]	STEMCELL	06005
TRIzol	Thermo Scientific	15596026
PI	MCE	HY-D0815
Recombinant TNF-α protein	R&D	410-MT-050/CF
Recombinant SFRP5 protein	R&D	7195-SF-050
Foxy-5	MCE	HY-P1416
Cultrex Organoid Harvesting Solution	R&D	700-100-01
DAPI	R&D	5748/50
5-ASA	Sigma-Aldrich	A3537
FD4	Sigma-Aldrich	60842-46-8
Critical commercial assays		
PrimeScript RT reagent kit	Takara	RR047A
SYBR Green qPCR Mix	Takara	
ELISA kit (TNF-α)	BOSTER	EK0527
ELISA kit (IL-6)	BOSTER	EK0411
ELISA kit (IL-17A)	BOSTER	EK0431
ELISA kit (IL-1β)	BOSTER	EK0394
ELISA kit (I-FABP)	BOSTER	EK1622
ELISA kit (SFRP5)	BOSTER	EK1472
In Situ Cell Death Detection Kit	Roche Diagnostics	12156792910
QIAamp UCP Pathogen Mini Kit	QIAGEN	50214
Experimental models: Cell lines		
Caco2 cells	ATCC	CBP60025

(*Continued on next page*)

Continued

REAGENT or RESOURCE	SOURCE	IDENTIFIER
Experimental models: Organisms/strains		
Wild-type mice (C57BL/6J)	Gempharmatech Co., Ltd	N/A
Mouse colonic organoids	This paper	N/A
Oligonucleotides		
Human *SFRP5* Forward : GTGCTGCACATGAAGAATGGC	This paper	N/A
Human *SFRP5* Reverse : GCCCCGTAGAAGAAAGGGT	This paper	N/A
Human *GAPDH* Forward : GGAGCGAGATCCCTCCAAAAT	This paper	N/A
Human *GAPDH* Reverse : GGCTGTTGTCATACTTCTCATGG	This paper	N/A
Mice *SFRP5* Forward : GAGATCAAGATAGACAACGGGGA	This paper	N/A
Mice *SFRP5* Reverse : TTGCGCTTTAAGGGGCCTG	This paper	N/A
Mice *TNF-α* Forward : CAGGCGGTGCCTATGTCTC	This paper	N/A
Mice *TNF-α* Reverse : CGATCACCCCGAAGTTCAGTAG	This paper	N/A
Mice *IL-6* Forward : TCTATACCACTTCACAAGTCGGA	This paper	N/A
Mice *IL-6* Reverse : GAATTGCCATTGCACAACTCTTT	This paper	N/A
Mice *IL-17A* Forward : GGCCCTCAGACTACCTCAAC	This paper	N/A
Mice *IL-17A* Reverse : TCTCGACCCTGAAAGTGAAGG	This paper	N/A
Mice *IL-1β* Forward : GAAATGCCACCTTTTGACAGTG	This paper	N/A
Mice *IL-1β* Reverse : TGGATGCTCTCATCAGGACAG	This paper	N/A
Mice *GAPDH* Forward : TGACCTCAACTACATGGTCTACA	This paper	N/A
Mice *GAPDH* Reverse : CTTCCCATTCTCGGCCTTG	This paper	N/A
Software and algorithms		
ImageJ software	ImageJ software	N/A
SPSS 23.0	IBM SPSS software	N/A
GraphPad Prism 9	GraphPad Software	N/A
Other		
rAAV9-SFRP5	Genechem Co., Ltd.	N/A

EXPERIMENTAL MODEL AND STUDY PARTICIPANT DETAILS

Human participants

The participants were collected from three groups, including CD patients [CD group] and non-CD patients [colon cancer, NL group] and healthy controls [HC group]. The inclusion criteria for patients with colon cancer: (1) pathologically diagnosed with colon cancer and underwent radical surgery; and (2) no concomitant malignant tumors of other tissue origins. The exclusion criterion was patients whose clinical data were incomplete. The inclusion criteria for patients with CD: (1) had a previous medical history and examination consistent with the diagnosis of CD; and (2) presented with diseased bowels and underwent surgical resection. The exclusion criteria were patients whose clinical data were incomplete and who were suffering from other immune system diseases. Based on the

inclusion and exclusion criteria, 18 each of CD patients, colon cancer patients and healthy controls were included in this study and the general clinical information was provided in Table S1. The study was approved by the Ethics Committee of Bengbu Medical University, and the application approval number was 2020-044. The specimens and clinical data were obtained with the consent of the patients, who signed an informed consent form.

Peripheral blood samples [5 mL] were obtained from all the participants. While the diseased and normal intestine [samples at the resection margin; 1 × 1×1 size] and its adjacent MAT [10 g], as well as the subcutaneous and omental adipose tissue [5 g], were collected from CD and colon cancer patients who underwent surgical resection. The specimen nomenclature for paired normal/diseased mesentery and intestine tissues was provided in Table S2. The intestine and MAT samples were divided equally into two parts: one was immediately stored in liquid nitrogen for molecular level testing, and the other was fixed with 10% formalin for the histopathological analysis, while the subcutaneous and omental adipose tissue were mixed only for histological experiment. Serum was separated from peripheral blood and immediately frozen at −80°C.

Mice

Male C57BL/6J mice [wild-type, WT] aged 6–8 weeks were purchased from Gempharmatech Co., Ltd [Nanjing, Jiangsu, China] and maintained in an SPF environment [the sex has no effect on intestinal inflammation]. The temperature was controlled at 23 ± 2°C without noise stimulation. The mice were fed and watered freely. The study was approved by the Ethics Committee of Bengbu Medical University, and the application approval number was 2021-226.

Mouse colonic organoids

Mouse colonic organoids were cultured using a previously reported protocol [Method S1]. A two-part *ex vivo* experiment was performed using an organoid model. The first part observed the effect of SFRP5 on TNF-α-induced intestinal epithelial cell apoptosis.[7,45] Briefly, on the fourth day after transmission, the organoids were pretreated with recombinant SFRP5 protein [0.5 μg/mL] for 30 min and then stimulated with TNF-α [10 ng/mL] for 12 h. The second part assessed the role of Wnt5a signaling in the effect of SFRP5 on the apoptosis of intestinal epithelial cells. Thirty minutes before TNF-α stimulation, the organoids were pretreated with SFRP5 and a Wnt5a-specific agonist [Foxy-5, 100 μM]. After the experiment, the organoids were collected for follow-up testing.

Caco2 cells

Caco2 cells were obtained from American Type Culture Collection [ATCC] and have been verified by short tandem repeat [STR] and are free of mycoplasma contamination. The mechanism of the antiapoptotic effect of SFRP5 on enterocytes was explored in Caco2 cells. The Caco2 cells were divided into four groups: the NC, TNF-α, TNF-α+SFRP5 and TNF-α+SFRP5+Foxy-5 groups. The NC group underwent normal culture. The cells in the TNF-α group were subjected to TNF-α [10 ng/mL] stimulation for 12 h, and the cells in the TNF-α+SFRP5 group were pretreated with recombinant SFRP5 protein [0.5 μg/mL] for 30 min and then stimulated with TNF-α for 12 h. In the TNF-α+SFRP5+Foxy-5 group, the cells were pretreated with SFRP5 and the Wnt5a-specific agonists [Foxy-5, 100 μM] for 30 min before TNF-α stimulation for 12 h. The experiment was repeated at least three times. After the experiment, the cells were collected for subsequent experiments.

METHOD DETAILS

Animal experimental design

The 2,4,6-trinitrobenzenesulfonic acid [TNBS]-induced colitis was established as a CD mouse model, and the modeling method was described in the Method S2. The animal experiments were performed in two parts: one part observed the effects of SFRP5 upregulation on CD-like colitis and intestinal barrier dysfunction, and the other part was assessed the effect of Wnt5a signaling on the action of SFRP5. The first part of the experiment consisted of five groups [N = 6]: WT, WT + SFRP5, TNBS, TNBS+SFRP5 and TNBS+5-aminosalicylic acid [5-ASA]. The mice received an intraperitoneal injection of an adeno-associated virus [rAAV9-SFRP5, 0.2 mL, 1×10^{11} vg, once] to upregulate SFRP5 expression in the MAT, and the remaining groups received the vehicle virus. The mice in the TNBS+SFRP5 group underwent TNBS modeling 4 weeks after the rAAV9-SFRP5 intervention, whereas the mice in the TNBS+5-ASA group received 5-ASA at a dose of 100 mg/kg/d [gavage, 0.2 mL] after TNBS modeling. All the mice were sacrificed 7 days after TNBS stimulation.

The second part of the experiment consisted of four groups [N = 6]: WT, TNBS, TNBS+SFRP5, and TNBS+SFRP5+Foxy-5. Six mice were included in each group. The interventions for the first three groups were the same as those in the first part of the experiment. The fourth group of mice was intraperitoneally injected with the Wnt5a-specific agonist [Foxy-5, 0.2 mL, 2 mg/kg/every other day] beginning 4 weeks before TNBS stimulation and continuing until the end of the experiment, for a total of 18 treatments.[46]

Animal specimen collection and processing

Body weight was measured and disease activity index [DAI] scores were assessed daily.[47] Fresh specimens of the mesenteric lymph nodes [MLNs], liver and spleen were collected after the mice were sacrificed by cervical dislocation under anesthesia. While, the plasma, colon and its adjacent MAT were obtained. After the length of the colon was measured and macroscopic histologic scoring

was performed,[20] the tissue was dissected into two segments along the longitudinal axis; one segment of the colon, mesentery, and serum was stored at −80°C, and the other segment was fixed with 10% formalin.

Endoscopic colitis score

Colonic lesions in mice were evaluated by endoscopy and the item as follows: thickening of the colon, changes in the vascular pattern, fibrin visible, granularity of the mucosal surface and consistency of the stool. Scores for each item ranged from 0 to 3, with higher score indicating more severe colitis.[48,49]

Histological analysis

As reported before,[50] the colon tissues of the mice were cut into 4 μm thick section, and the severity of colitis was quantified based on hematoxylin-eosin [H&E] staining [0 to 4 scores].

Immunohistochemical [IHC] staining

As previously reported,[13] the 4 μm sections were deparaffinized, antigens were exposed, endogenous peroxidases were blocked, blocking with serum was performed, then incubated with an anti-SFRP5 antibody [1:500] at 4°C overnight, followed by an incubation with goat anti-rabbit IgG H&L [HRP] antibody [1:1000] and color rendering with diaminobenzidine, and then the nuclei were stained with hematoxylin. The IHC results were quantified using ImageJ software.

RT-qPCR

As reported,[15] total RNA was obtained with TRIzol, and then the RNA was reverse transcribed into cDNA. Finally, PCR amplification was performed. GAPDH was used as a reference gene, and the $2^{-\Delta\Delta Ct}$ method was used for relative quantitative analysis.

ELISA

The levels of TNF-α, IL-6, IL-17A and IL-1β in mouse colonic mucosa, intestinal fatty acid binding protein [I-FABP] in mouse plasma, and SFRP5 in human serum were detected using ELISA kits according to the manufacturers' procedures.

Immunofluorescence [IF] analysis

IF staining was routinely performed as previously reported.[51] Briefly, the paraffin sections [mouse colon tissues and organoids; 4 μm] were incubated with anti-C-caspase3 [1:400], anti-ZO-1 [1:500], anti-Claudin-1 [1:200] or anti-Wnt5a antibodies [1:200] at 4°C overnight, followed by an incubation with Alexa Fluor555/FITC-labelled goat anti-rabbit/mouse IgG H&L antibodies [1:1000] and staining with DAPI. The images were obtained with a laser confocal microscope [FLUOVIEW FV300, Olympus].

TUNEL staining

The level of apoptosis was assessed by TUNEL staining using an *In Situ* Cell Death Detection Kit, and the nuclei were stained with DAPI. The average number of TUNEL-positive epithelial cells per villus in 4 random fields in each slice was determined.[52]

Western bloting [WB]

The levels of target proteins in the mesentery, intestinal mucosa and organoids were quantitatively analyzed via WB as described previously.[20,53] In short, the extracted total protein was quantified, denatured, separated by SDS-PAGE and transferred to PVDF membranes. The membranes were blocked and incubated with anti-SFRP5 [1:1000], anti-C-caspase3 [1:1000], anti-ZO-1 [1:1000], anti-Claudin-1 [1:1000], anti-Wnt5a [1:500], anti-JNK [1:1000], anti-*p*-JNK [1:1000] or anti-Bcl2 [1:2000]. Subsequently, goat anti-rabbit/mouse IgG H&L [HRP] antibodies [1:2000] were added, followed by exposure and development.

PI staining

Epithelial cell death in mouse colonic organoids was analyzed using PI staining, as previously described.[54] Briefly, the PI solution [diluted in PBS] was added to the organoid growth medium at a final concentration of 10 μg/mL and incubated for 30 min at 37°C with 5% CO_2. Finally, the proportion of PI-positive cells in each organoid was analyzed using a laser confocal microscope [FLUOVIEW FV300].

FD4 permeability analysis *in vivo*

Briefly, the mice were fasted for 4 h and then orally administered FD4 [600 mg/kg]. Four hours later, the mice were sacrificed, plasma was collected via cardiac puncture, and the levels of FD4 were determined using a fluorometry assay.[55]

TEER measurement *in vivo*

TEER was used to assess the permeability of mouse colon tissue, as previously reported.[55] Fresh mouse colon tissue was cut to a size of 2.8 mm × 11 mm, placed into a rectangular slider [Chamber Systems P2304; Warner Instruments] and loaded into the Ussing chamber system [Chamber Systems CSYS-4HA]. Krebs buffer was added to the two chambers of the system with 10 mM glucose on the serosal side and 10 mM mannitol on the luminal side. After 15 min of tissue equilibration, the potential difference was maintained

at zero by applying an appropriate short-circuit current via automatic voltage clamp control, and then the colonic TEER value was measured.

Measurement of 16S rDNA

As described previously,[56] microbial DNA was isolated from mouse plasma samples using the QIAamp UCP pathogen mini kit, followed by PCR amplification of 16S rDNA. The primer sequences were as follows: forward [8F: 5′-AGTTTGATCCTGGCTCAG-3’] and reverse [515R: 5′-GWATTACCGCGGCKGCTG-3’]. The probe sequence was [338P: 5′-FAMGCTGCCTCCCGTAGGAGT-BHQ1-3’].

Bacterial translocation

According to previous reports,[28] the proportion of ectopic intestinal bacteria was determined by aseptically isolating and culturing mesenteric lymph nodes [MLNs] and liver and spleen tissues from mice, and more than 10^2 colony-forming units per gram of tissue was considered a positive result.

TEM analysis

Using a previously reported method,[55] fresh mouse colon tissues [1 mm × 1 mm] were cut into thin sections and fixed with 2.5% glutaraldehyde. Subsequently, the ultrastructure of intercellular junctions was observed under a TEM [Hitachi H-600, Hitachi].

Ex vivo FD4 permeability assay

The permeability of mouse colonic organoids to FD4 was determined as previously described.[57] Matrigel was lysed with 500 μL of Cultrex organoid harvesting solution by shaking at 4°C for 20 min. The colonic suspension was collected and centrifuged at 500 × g for 5 min, the supernatant was discarded, and the remaining cells were resuspended in 30 μL of FD4 solution [diluted in complete medium with growth factors] at a concentration of 2 mg/mL and immediately imaged with a laser confocal microscope [FLUOVIEW FV300]. Finally, the fluorescent signal was quantified using ImageJ software.

TEER measurement in ex-vivo

As reported previously,[58] the upper chamber of the Transwell insert [24-well plate, 0.4 mm, Corning] was covered with Matrigel solution and incubated for at least 1 h at room temperature. The organoids were prepared as small fragments and resuspended in organoid growth medium, after which 0.3 mL was added to the membrane plate. One membrane plate was supplemented with only growth medium as a blank control. Next, organoid growth medium [1.4 mL] was added to the lower chamber of the Transwell insert. Electronic resistance [ohm] was assessed using an EVOM2 transepithelial resistance meter [World Precision Instruments Inc. Sarasota, Florida, USA]. TEER values were calculated by the following equation: TEER = [ohms (sample) - ohms (control)] × 0.33 cm^2.

QUANTIFICATION AND STATISTICAL ANALYSIS

Statistical analysis was performed with SPSS 23.0 and GraphPad Prism 9. The measurement data are presented as the mean ± standard deviation [SD] and one-way ANOVA [Tukey’s multiple test] was used for comparisons between groups. Enumeration data were expressed as the composition ratio, and comparisons between groups were analyzed with the chi-square test. A p value less than 0.05 was considered to indicate a significant difference.